encit 2020
18th Brazilian Congress of Thermal Sciences and Engineering
November 16–20, 2020 (Online)

ENC-2020-0809
STRUCTURAL ELASTO-VISCOPLASTIC FLOW: A NUMERICAL STUDY

Vitor Dal Bó Abella
Sérgio Frey
Departament of Mechanical Engineering, Federal University of Rio Grande do Sul - Rua Sarmento Leite, 425 – 90050-170 – Porto Alegre, RS, Brazil
vitor.abella@mecanica.ufrgs.br, frey@mecanica.ufrgs.br

Natan A. de Oliveira
Farroupilha Federal Institute – IFFar Panambi - Rua Erechim, Panambi, RS 90830-990, Brazil
natan.oliveira@iffarroupilha.edu.br

Abstract. *This article carries on a stabilized finite element approximations for inertialess flow of structured elasto-viscoplastic materials. The mechanical modeling is based on the classic mass and momentum conservation equations for incompressible materials coupled with a viscoelastic equation that takes into account the dependence of relaxation time and viscosity on Rheology. To approximate this mechanical model, a stabilized finite element formulation is applied in terms of the extra stress tensor, the pressure field, and velocity vector. Numerical results intend to perform a numerical investigation of the influence of the yield stress on the flow pattern.*

Keywords: *viscoplasticity, structured fluids, elasticity, contraction flow, stabilized finite element method*

1. INTRODUCTION

The study of non-Newtonian fluids is of scientific and industrial relevance since their significant presence in industrial applications. To list only a few, there are polymeric extruder flow in the plastic industry, manufacture of gels, shampoos and inks in the cosmetic industry, and perforation muds in the oil industry (Mahmood *et al.*, 2017).

According to Bingham (1922), when the viscoplastic behavior is present in the fluid, the yield stress must be achieved to the fluid start to flow. If the internal stress is lower than the yield stress, the material doesn't flow. Those regions on which yield stress is not surpassed are called unyielded regions, and the interface between unyielded and yielded regions is known as yield surfaces. Barnes (1999a,b) claimed that the *yield stress* doesn't exist, contradicting the classical definition. There is a huge increase (but finite) in the viscosity near the yield stress. This new definition created the so-called apparent yield stress fluids. Besides, studies verified elastic behavior within unyielded regions – see, for instance, (Gueslin *et al.*, 2006; Putz *et al.*, 2008; Sikorski *et al.*, 2009), and reference therein. Also, elasto-viscoplastic materials may present thixotropic behavior (Balmforth *et al.*, 2014; Coussot, 2014).

Complex flows are frequent in industrial processes and Nature. Accidents imposed by complex geometries induce to geometric nonlinearities, such as back-flow recirculations and flow detachments. In the particular of Non-Newtonian flows, their material equations add material nonlinearity to the mechanical modeling employed. Complex fluids, such as elasto-viscoelastic and thixotropic ones, induce striking effects when flowing through complex geometries – such as memory and non-zero normal stress differences.

In the last decade, some authors have investigated numerically and proposed constitutive equations for this class of material. Nassar *et al.* (2011) simulated elasto-viscoplastic materials in axisymmetric expansion-contraction flows using a model based on the one proposed by de Souza Mendes and Dutra (2004). Belblidia *et al.* (2011) approximated an axisymmetric expansion-contraction flow through a 4:1:4 contraction-expansion channel, with the BWW model introduced by the authors. Santos *et al.* (2014) studied the elasto-viscoplastic flow through a duct subjected to an expansion-contraction using the model proposed by de Souza Mendes (2011). Link *et al.* (2015) computed a thixotropic flow over a 1:4 sudden expansion using the model introduced by de Souza Mendes (2011). Fraggedakis *et al.* (2016) compared five recent proposed elasto-viscoplastic models proposed by Saramito (2007, 2009); Park and Liu (2010); Belblidia *et al.* (2011) in the flow around a falling spherical particle. López-Aguilar *et al.* (2016) contrasted the models proposed by López-Aguilar *et al.* (2014) and de Souza Mendes (2011) in thixotropic flow over an axisymmetric contraction-expansion. Oishi *et al.* (2017) evaluated the avalanche-effect of thixopic elasto-vicoplastic flows over an inclined plane using de Souza Mendes and Thompson (2013) model. López-Aguilar *et al.* (2018) simulated a thixotropic elasto-viscoplatic fluid flow over a circular contraction-expansion using a new model called $BMP+\_\tau_p$ and the model from de Souza Mendes (2011). Oishi *et al.* (2020) solved the collision of elasto-viscoplastic drops in vertical plane using a model similar to Saramito (2009).

The current article uses the thixotropic equation proposed by de Souza Mendes (2009) to predict elastic, viscoplastic, and shear-thinning effects in a yield stress material that flows through a two to one sudden contraction. The model is approximated by a three-field Galerkin least-squares–like method, in terms of extra stress, pressure, and velocity, aiming at allowing the use of Lagrangean finite elements, and to improve the convergence of Galerkin method.

2. MATHEMATICAL FORMULATION

2.1 Elasto-viscoplastic model

To predict elasto-viscoplasticity flow, in this article we adopt the thixotropic material equation introduced in de Souza Mendes (2011). According to this equation, the material is modeled as a structural fluid, i.e., the elasto-viscoplasticity is defined in terms of the structuring level of material microstructure. Applying the elastic-viscous-split-stress scheme (EVSS) (Rajagopalan *et al.*, 1990), this equation is mathematically described by:

$$\boldsymbol{T} = \boldsymbol{\tau} + \mathfrak{T} \tag{1}$$

$$\boldsymbol{\tau} + \theta_s(\lambda)\overset{\nabla}{\boldsymbol{\tau}} = 2\eta_s(\lambda)\left(\mathbf{D}(\mathbf{u})\right) \tag{2}$$

$$\mathfrak{T} = 2\eta_\infty \boldsymbol{D}(\boldsymbol{u}) \tag{3}$$

where η_∞ is the solvent viscosity, η_s is the structural viscosity, $\mathbf{D}(\mathbf{u})$ is the strain rate tensor whose magnitude is given by $\dot{\gamma} \equiv (\frac{1}{2}\,\mathrm{tr}\,\mathbf{D}(\mathbf{u})^2)^{1/2}$, $\boldsymbol{T}$ is the extra stress, $\mathfrak{T}$ and $\boldsymbol{\tau}$ are respectively the pure viscous and the non-newtonian part of $\boldsymbol{T}$, and $\overset{\nabla}{\boldsymbol{\tau}}$ denotes the upper-convected derivative of $\boldsymbol{\tau}$, defined as:

$$\overset{\nabla}{\boldsymbol{\tau}} = (\nabla\boldsymbol{\tau})\mathbf{u} - (\nabla\mathbf{u})\boldsymbol{\tau} - \boldsymbol{\tau}(\nabla\mathbf{u})^T \tag{4}$$

The structural relaxation time, θ_s, the structural shear elastic modulus G_s and the structural viscosity η_s are a function of the structuring level λ as follows:

$$\theta_s(\lambda) = \frac{\eta_s(\lambda)}{G_s(\lambda)} \tag{5}$$

$$G_s(\lambda) = G_0 \exp\left(m\left(\frac{1}{\lambda} - 1\right)\right) \tag{6}$$

$$\eta_s(\lambda) = \left(\frac{\eta_0}{\eta_\infty}\right)^\lambda \eta_\infty \tag{7}$$

where G_0 is the structural elastic modulus of a fully structured material and m is an arbitrary positive parameter that controls the sensitivity of G_s with respect to λ, $m = \frac{\partial G_s}{\partial \lambda}$. Another parameter to identify the fluid is the elastic parameter $\theta_0 = \frac{\eta_0}{G_0}$.

The structuring level λ is obtained by the integration of an evolution equation correlating the substantial derivative of the structuring level with the imbalance of the build-up and breakdown rates, de Souza Mendes (2011):

$$\frac{D\lambda}{Dt} = \frac{1}{t_{eq}}\left[(1-\lambda) - (1-\lambda_{eq})\frac{\lambda}{\lambda_{eq}}\right] \tag{8}$$

where the thixotropic equilibrium time, t_{eq}, characterizes the time of change of λ once the stress levels change.

A useful elasto-viscoplastic model can be obtained from the thixotropic model defined by Eq. (2)-(8) assuming that the structuring level changes infinitely fast, $\dot{\lambda} \to \infty$. Physically, it means that the structuring level achieves another equilibrium configuration instantaneously ($t_{eq} \to 0$) when the stress profile changes. Assuming that the material has no thixotropic behavior, the evolution Eq. (8) is trivially satisfied and all Rheological properties are in equilibrium state, e.g., $\lambda = \lambda_{eq}$, $\eta_s = \eta_{eq}$, $G_s = G_{eq}$ and $\theta_s = \theta_{eq}$. Then, taking the logarithmic of Eq. (7) the following expression is obtained:

$$\lambda(\dot{\gamma}) = \frac{\ln \eta_s(\dot{\gamma}) - \ln \eta_\infty}{\ln \eta_0 - \ln \eta_\infty} \tag{9}$$

According to Eq. (9), λ is thus a scalar-valued distribution that ranges from 0 to 1 and maps the structuring level of the microstructure. For $\lambda = 1$ the material is fully-structured, the model predicts elastic body behavior and, for $\lambda = 0$ the material is fully unstructured with the model predicting a pure viscous behavior. For $0 < \lambda < 1$, the model predicts a viscoelastic behavior. This formulation assumes that there is a one-to-one relationship between the structuring level and viscosity levels.

In this work, to model the viscoplasticity, the following expression for the equilibrium viscosity was employed, from de Souza Mendes and Dutra (2004):

$$\eta_{eq}(\dot{\gamma}) = \left[1 - \exp\left(-\frac{\eta_0 \dot{\gamma}}{\tau_0}\right)\right]\left\{\frac{\tau_0}{\dot{\gamma}} + K\dot{\gamma}^{n-1}\right\} + \eta_\infty \tag{10}$$

where τ_0 is the yield stress, K the consistency index, and n the power-law coefficient.

2.2 Balance equations and problem statement

The fluid is assumed to be incompressible, the flow is steady and the gravitational force is neglectable. Let the flow occurs through an open domain $\Omega \subset \Re^2$. The mass and momentum balance equations are written as:

$$\mathrm{div}\,\mathbf{u} = 0 \quad \text{in} \;\; \Omega \tag{11}$$

$$\rho(\nabla\mathbf{u})\mathbf{u} = -\nabla p + \mathrm{div}\,\boldsymbol{\tau} + 2\eta_\infty \mathrm{div}(\boldsymbol{D}(\mathbf{u})) \quad \text{in} \;\; \Omega \tag{12}$$

where $\mathbf{u}$ is the velocity vector, p is the pressure and $\boldsymbol{\tau}$ is defined in Eq. (2).

The geometry is a planar 2:1 sudden contraction. The no-slip and impermeability hypotheses are considered on the wall. At the outlet, free traction condition is applied, $\boldsymbol{Tn} = (-p\boldsymbol{I} + \boldsymbol{\tau} + 2\eta_s(\lambda)\,(\mathbf{D}(\mathbf{u})))\boldsymbol{n} = \mathbf{0}$, and at the inlet, a flat profile $u_1 = U$ is set and, at the centerline symmetric boundary conditions are adopted. The problem statement is represented in Fig. 1.

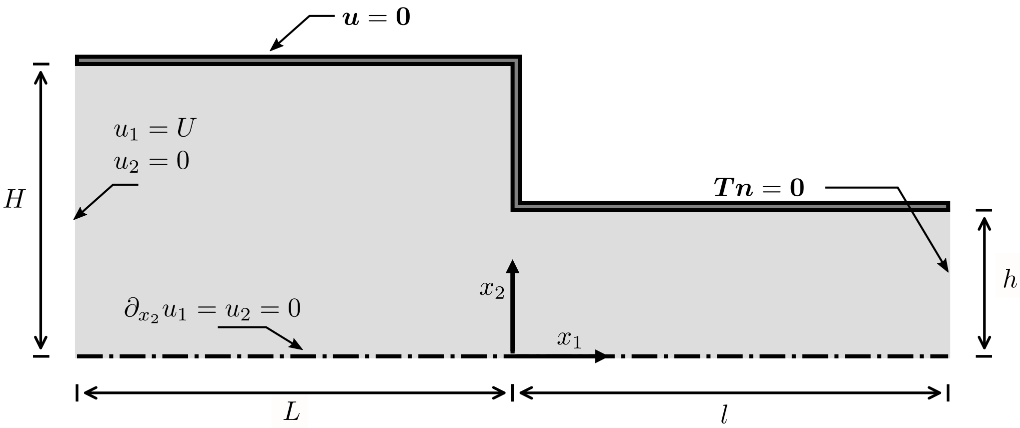

Figure 1: The problem statement.

3. NUMERICAL METHOD

Let $\Omega \subset \mathbb{R}$ be the domain of the model with its surroundings $\Gamma = \partial\Omega$. The problem is defined by a set of coupled equations that aim to find $\mathbf{u}(\mathbf{x}) = (u_1(\mathbf{x}), u_2(\mathbf{x})) \in C^2(\Omega)^2$, $P(\mathbf{x}) \in C^1(\Omega)$ and $\boldsymbol{\tau}(\mathbf{x}) \in C^1(\Omega)$ satisfying:

$$\mathrm{div}\,(\mathbf{u}) = 0, \qquad \text{in} \quad \Omega, \tag{13}$$

$$\rho(\nabla\mathbf{u})\mathbf{u} = -\nabla p + \mathrm{div}\,(2\eta_\infty \mathbf{D}(\mathbf{u})) + \mathrm{div}\,(\boldsymbol{\tau}), \qquad \text{in} \quad \Omega, \tag{14}$$

$$\boldsymbol{\tau} + \theta_s(\lambda)\overset{\triangledown}{\boldsymbol{\tau}} = 2\eta_s(\lambda)\mathbf{D}(\mathbf{u}), \qquad \text{in} \quad \Omega, \tag{15}$$

$$\mathbf{u} = \mathbf{u}_g, \qquad \text{on} \quad \Gamma_g^{\boldsymbol{u}}, \tag{16}$$

$$\boldsymbol{\tau} = \boldsymbol{\tau}_g \qquad \text{on} \quad \Gamma_g^{\boldsymbol{\tau}} \tag{17}$$

$$\mathbf{0} = (-p\boldsymbol{I} + \boldsymbol{\tau} + 2\eta_s(\lambda)\,(\mathbf{D}(\mathbf{u})))\boldsymbol{n} \qquad \text{on} \quad \Gamma_h \tag{18}$$

The numerical scheme employed to solve the problem is finite element multifield Galerkin least-squares in terms of velocity, pressure and extra stress proposed by Franca and Frey (1992). In order to accomplish the variational formulation of Equations (13)-(18), the space of functions are defined:

$$\mathbf{V} = \{\mathbf{v} : \Omega \to \mathbb{R}^2 \mid \mathbf{v} \in H^1(\Omega)^2 \text{ and } \mathbf{v} = \mathbf{0} \text{ on } \Gamma_g^{\mathbf{u}}\} = H_0^1(\Omega)^2 \quad (19)$$

$$Q = \left\{q : \Omega \to \mathbb{R} \mid q \in L^2(\Omega),\ \int_\Omega q \mathrm{d}\Omega = 0\right\} = L_0^2(\Omega) \quad (20)$$

$$\mathbf{\Sigma} = \{\mathbf{S} : \Omega \to \mathbb{R}^{2\times 2} \mid \mathbf{S} \in L^2(\Omega)^{2\times 2}\} = L^2(\Omega)^{2\times 2} \quad (21)$$

where $\mathbf{V}$, Q e $\mathbf{\Sigma}$ are space of functions related respectively to $\mathbf{u}$, P and $\boldsymbol{\tau}$.

The mathematical problem is defined as following:

Find $(\mathbf{u}^h, P^h, \boldsymbol{\tau}^h) \in (\mathbf{V}^h, Q^h, \mathbf{\Sigma}^h)$, *such that:*

$$B(\mathbf{u}^h, P^h, \boldsymbol{\tau}^h; \mathbf{v}^h, q^h, \mathbf{S}^h) = 0,\ \forall(\mathbf{v}^h, q^h, \mathbf{S}^h) \in (\mathbf{V}^h, Q^h, \mathbf{\Sigma}^h). \quad (22)$$

where

$$\begin{aligned} B(u_i^h, P^h, \tau_{ij}^h; v_i^h, q^h, S_{ij}^h) = &\int_\Omega \partial_{x_i} u_i^h q^h \mathrm{d}\Omega - \int_\Omega \rho \left(\partial_{x_j} u_i{}^h\right) u_i^h v_j{}^h d\Omega \\ &+ \int_\Omega P^h \partial_{x_i} v_i^h \mathrm{d}\Omega - 2\eta_\infty \int_\Omega D(u^h)_{ij} : D(v^h)_{ij} \mathrm{d}\Omega - \int_\Omega \tau_{ij}^h : D(v^h)_{ij} \mathrm{d}\Omega \\ &+ \int_\Omega \tau_{ij}^h : S_{ij}^h \,\mathrm{d}\Omega + \int_\Omega \theta_s(\lambda) \overset{\triangledown}{\tau}_{ij}{}^h : S_{ij}^h \,\mathrm{d}\Omega - \int_\Omega 2\eta_v(\lambda) D(u^h)_{ij} : S_{ij}^h \,\mathrm{d}\Omega \\ &+ \delta(Re_K) \int_\Omega \partial_{x_i} u_i^h \cdot \partial_{x_i} v_i^h \mathrm{d}\Omega \\ &+ \alpha(Re_K) \sum_{K \in \Omega^h} \int_{\Omega_K} (\partial_{x_i} P^h - \partial_{x_j} \tau_{ij}{}^h - 2\eta_\infty \partial_{x_j} D(u)_{ij}^h) \cdot \\ &\cdot (\partial_{x_i} q^h - \partial_{x_j} S_{ij}{}^h - 2\eta_\infty \partial_{x_j} D(v)_{ij}^h) d\Omega \\ &+ \beta \int_\Omega ((2\eta_s(\lambda))^{-1} \tau_{ij}{}^h + (2\eta_s(\lambda))^{-1} \theta_s(\dot\gamma) \overset{\triangledown}{\tau}{}_{ij}^h - D(u)_{ij}{}^h)) \cdot \\ &\cdot ((2\eta_s(\lambda))^{-1} S_{ij}{}^h + (2\eta_s(\lambda))^{-1} \theta_s(\lambda) \overset{\triangledown}{S}{}_{ij}^h - D(v)_{ij}{}^h)) d\Omega \end{aligned} \quad (23)$$

and its numerical parameters are:

$$\mathsf{Re}_K = \frac{\rho h_K ||\mathbf{u}^h||_0 m_k}{4\eta_e(\dot\gamma)} \quad (24)$$

$$\alpha(\mathsf{Re}_K) = \frac{h_K}{2||\mathbf{u}^h||_0} \zeta(\mathsf{Re}_K) \quad (25)$$

$$\delta(\mathsf{Re}_K) = \lambda_d ||\mathbf{u}^h||_0 h_K \zeta(\mathsf{Re}_K) \quad (26)$$

$$\zeta(\mathsf{Re}_K) = \begin{cases} \mathsf{Re}_K, & 0 < \mathsf{Re}_K < 1 \\ 1, & \mathsf{Re}_K > 1 \end{cases} \quad (27)$$

$$||\mathbf{u}^h||_0 = \left(\sum_{i=1}^N |u_i^h|^2\right)^{1/2} \quad (28)$$

$$m_k = \min\left\{\frac{1}{3}, 2C_k\right\} \quad (29)$$

$$C_k \sum_{K \in \Omega^h} h_K^2 ||\operatorname{div}(\mathbf{S}^h)||_{0,K}^2 \geq ||\mathbf{S}^h||_0^2, \quad \forall\, \mathbf{S}^h \in \mathbf{\Sigma}^h \quad (30)$$

where $||\cdot||_{0,K}$ is the norm $L^2(\Omega)$ restrict to an element K in the discretization, λ_d is a positive parameter, h_K is the mesh length and β is an arbitrary value greater than 0.

4. NONDIMENSIONALISATION OF EQUATIONS

As discussed in de Souza Mendes (2011), three shear rates mark important transitions in the flow curve, namely $\dot\gamma_0, \dot\gamma_1$, and $\dot\gamma_2$. The $\dot\gamma_0$ is the maximum shear rate in which the material remains at η_0. $\dot\gamma_1$ marks the beginning of the power-law region. Above $\dot{\gamma}_2$ the material structure is destroyed, representing the transition between power law to Newtonian.

$$\dot{\gamma}_0 = \frac{\tau_0}{\eta_0}\ ,\ \ \dot{\gamma}_1 = \left(\frac{\tau_0}{K}\right)^{1/n}\ ,\ \ \dot{\gamma}_2 = \left(\frac{\eta_\infty}{K}\right)^{1/(n-1)} \tag{31}$$

Using $\dot{\gamma}_1$, the equations are adimensionalized as proposed by de Souza Mendes (2007). The adimensional variables are defined as:

$$\begin{array}{llll} G^* = \dfrac{G}{\tau_0} & p^* = \dfrac{p}{\tau_0} & \eta^* = \dfrac{\eta\dot{\gamma}_1}{\tau_0} & \theta^* = \dot{\gamma}_1\theta \\ \boldsymbol{\tau}^* = \dfrac{\boldsymbol{\tau}}{\tau_0} & \dot{\boldsymbol{\gamma}}^* = \dfrac{\dot{\boldsymbol{\gamma}}}{\dot{\gamma}_1} & \mathbf{u}^* = \dfrac{\mathbf{u}}{\dot{\gamma}_1 h} & \boldsymbol{x}^* = \dfrac{\boldsymbol{x}}{h} \end{array} \tag{32}$$

and the adimensional balance equations, already considering inertialess flow:

$$\operatorname{div}^*(\mathbf{u}^*) = 0, \quad \text{in} \quad \Omega^*, \tag{33}$$

$$0 = -\nabla^* p^* + \operatorname{div}(2\eta^*_\infty \mathbf{D}(\mathbf{u}^*)) + \operatorname{div}(\boldsymbol{\tau}^*), \quad \text{in} \quad \Omega^*, \tag{34}$$

$$\boldsymbol{\tau}^* + \theta^*(\lambda)\overset{\triangledown}{\boldsymbol{\tau}^*} = 2\eta^*_s(\lambda)\mathbf{D}(\mathbf{u}^*), \quad \text{in} \quad \Omega^*, \tag{35}$$

$$\mathbf{u}^* = \mathbf{u}^*_g, \quad \text{on} \quad \Gamma^{\boldsymbol{u}^*}_g, \tag{36}$$

$$\boldsymbol{\tau}^* = \boldsymbol{\tau}^*_g \quad \text{on} \quad \Gamma^{\boldsymbol{\tau}^*}_g \tag{37}$$

$$(-p^*\boldsymbol{I} + \boldsymbol{\tau}^*)\boldsymbol{n} = \mathbf{0} \quad \text{on} \quad \Gamma_h \tag{38}$$

where the adimensional relaxation time, θ^*, elasticity modulus, G^*, and structural viscosity are defined as:

$$\theta^*(\lambda) = \frac{\eta^*_s(\lambda)}{G^*(\lambda)} \tag{39}$$

$$G^*(\lambda) = G^*_0 \exp\left[m\left(\frac{1}{\lambda} - 1\right)\right] \tag{40}$$

$$\eta^*_s = \left[1 - \exp\left(\eta^*_0\dot{\gamma}^*\right)\right]\left[\frac{1}{\dot{\gamma}^*} + \dot{\gamma}^{*(n-1)}\right] + \eta^*_\infty \tag{41}$$

The adimensional elastic parameter, θ^*_0, is defined as $\theta^*_0 = \frac{\eta_0}{G_0}\dot{\gamma}_1$.

5. RESULTS

Preliminary results intend to study the influence of the flow intensity, U^*, on the topology of the yield surfaces, the structuring level and the adimensional relaxation time. The rheological parameters of the fluid are $\theta^*_0 = 1.0 \times 10^2$, $m = 1.0 \times 10^1$, $G^*_0 = 1.0 \times 10^4$, $n = 5.0 \times 10^{-1}$, $\eta^*_0 = 1.0 \times 10^4$ and $\eta^*_\infty = 1.0 \times 10^{-2}$. The hypothesis of inertialess flow is considered. The computational domain is partitioned into a bi-linear Lagrangian finite element mesh for all primal variables with 5598 elements.

The Fig. 2 shows the yielded ($|\boldsymbol{\tau}| \geq \tau_0$) and unyielded ($|\boldsymbol{\tau}| < \tau_0$) regions. Due to the low-stress level, the unyielded regions experience the lowest strain rates, namely in the dead zones and in the plug flow along with the channel centerline. On the other hand, in the vicinity of the contraction and near the wall, where the deformation rates receive the greatest values, are the yielded zones. The increase of the flow intensity narrows the unyielded zones along x^*_1 and move it away from the contraction.

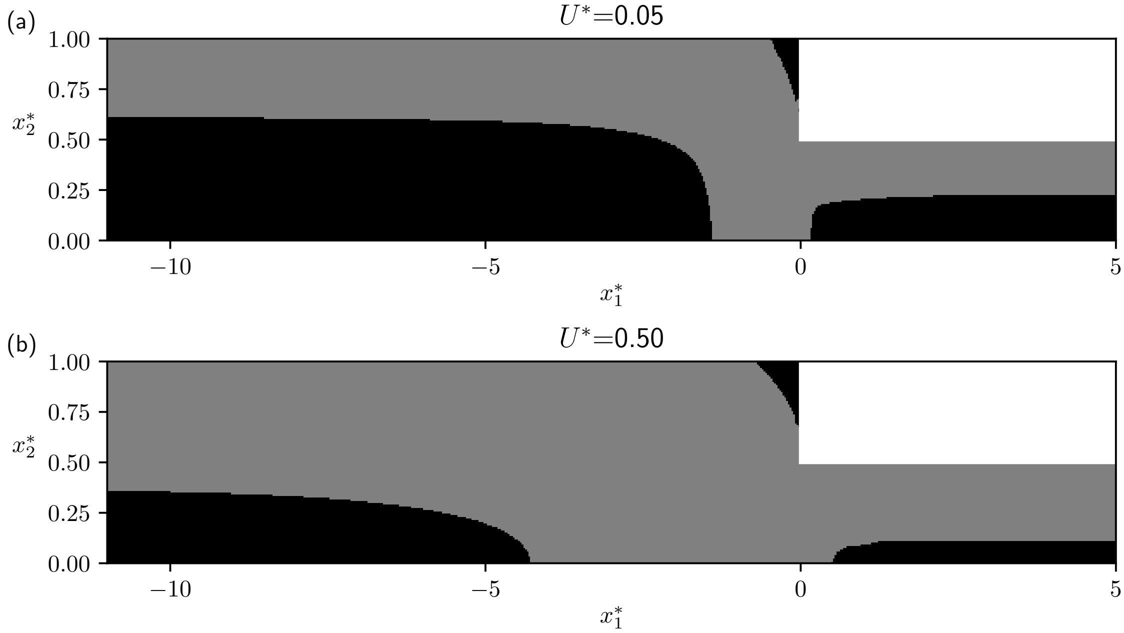

Figure 2: The effect of flow intensity on the yielded zones, (a) $U^* = 0.05$ and (b) $U^* = 0.50$. The zones in black the stress doesn't exceeds the yield stress, unyielded, and the yielded zones are in gray.

The topology of the structuring level is shown in the Fig. 3. Its results are in accordance with those of the yielded zones, Fig. 2. As expected, λ is higher inside the unyielded zones, because the stress is not enough to break the microestructure. When $U^* = 0.50$, there are higher strain rates near the wall and in the vinicity of the contraction, then the structuring level assumes lower values in those regions when compared to $U^* = 0.05$. Another remark is that for $U^* = 0.50$, the gradient of λ in the pre-contraction zone is smoother, because its unyielded zones also becomes yielded smoother in this region.

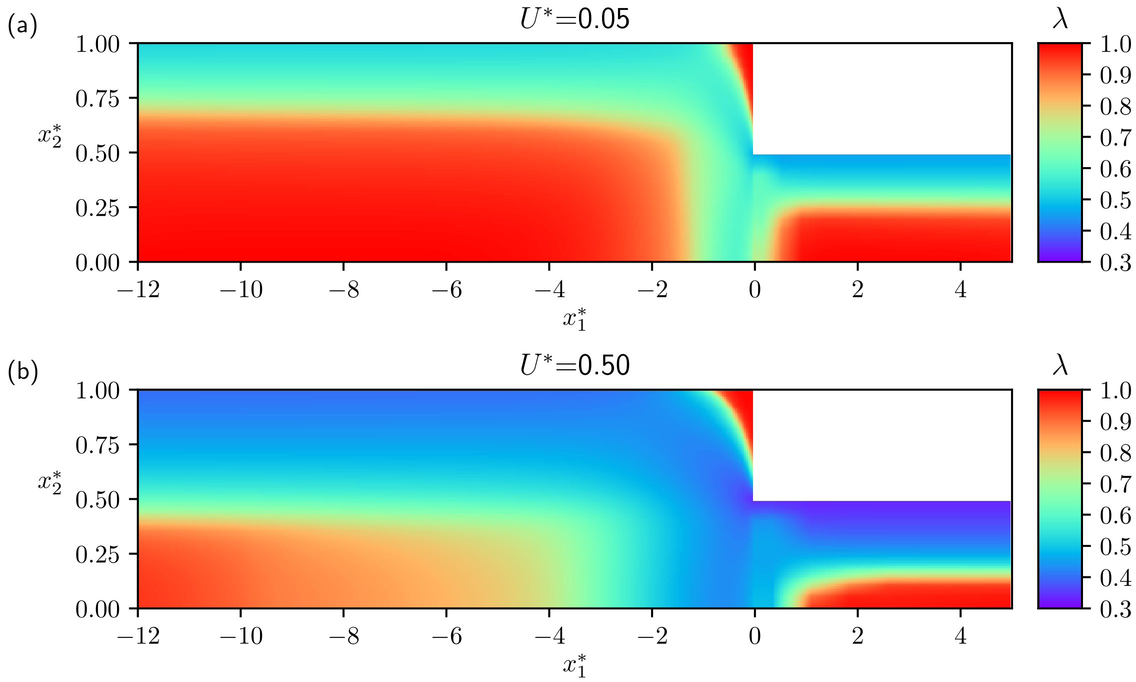

Figure 3: The effect of flow intensity on the structuring level, (a) $U^* = 0.05$ and (b) $U^* = 0.50$.

The 2D plot of θ^*, Fig. 4, shows the zones were the elasticity is present, i.e., those where θ^* is greater than zero. They are located inside and in the proximity of the unyielded zones. Far from the unyielded zones, the flow is purely viscous.

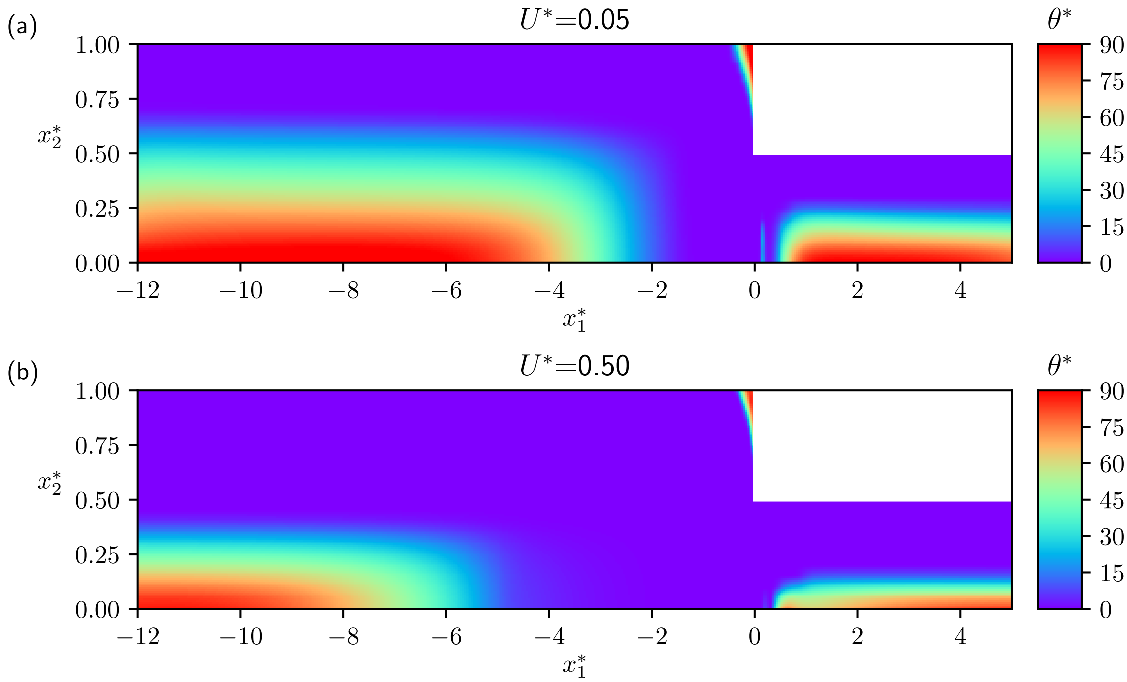

Figure 4: The effect of flow intensity on the relaxation time, (a) $U^* = 0.05$ and (b) $U^* = 0.50$.

6. CONCLUSIONS

The flow of an elasto-viscoplastic fluid is observed through a 2:1 axissymmetric contraction. It was verified that the flow intensity has a significant influence in the flow near the contraction. The increase of U^* shrinks the unyielded regions, where the yield surface marks the change on λ and θ^*. For further studies, the goal is to analyze the influence of the contraction ratio, θ_0^* and inertia on elasto-viscoplastic fluid flows.

7. ACKNOWLEDGMENTS

The author V. D. B. Abella thanks the financial support by CNPq and CAPES.

8. RESPONSIBILITY NOTICE

The author is the only responsible for the printed material included in this paper.

9. REFERENCES

Balmforth, N.J., Frigaard, I.A. and Ovarlez, G., 2014. "Yielding to stress: Recent developments in viscoplastic fluid mechanics". *Annual Review of Fluid Mechanics*, Vol. 46, No. 1, pp. 121–146.

Barnes, H.A., 1999a. "A brief history of the yield stress". *Appl. Rheol*, Vol. 9, No. 6, pp. 262–266.

Barnes, H.A., 1999b. "The yield stress - a review or $\pi\alpha\nu\tau\alpha\ \rho\varepsilon\iota$ - everything flows?" *Journal of Non-Newtonian Fluid Mechanics*, Vol. 81, No. 1-2, pp. 133–178.

Belblidia, F., Tamaddon-Jahromi, H.R., Webster, M.F. and Walters, K., 2011. "Computations with viscoplastic and viscoelastoplastic fluids". *Rheologica Acta*, Vol. 50, No. 4, pp. 343–360.

Bingham, E.C., 1922. *Fluidity and plasticity*, Vol. 2. McGraw-Hill.

Coussot, P., 2014. "Yield stress fluid flows: A review of experimental data". *Journal of Non-Newtonian Fluid Mechanics*, Vol. 211, pp. 31–49.

de Souza Mendes, P.R., 2007. "Dimensionless non-Newtonian fluid mechanics". *Journal of Non-Newtonian Fluid Mechanics*, Vol. 147, No. 1-2, pp. 109–116.

de Souza Mendes, P.R., 2009. "Modeling the thixotropic behavior of structured fluids". *Journal of Non-Newtonian Fluid Mechanics*, Vol. 164, No. 1-3, pp. 66–75.

de Souza Mendes, P.R., 2011. "Thixotropic elasto-viscoplastic model for structured fluids". *Soft Matter*, Vol. 7, pp.

2471–2483.

de Souza Mendes, P.R. and Thompson, R.L., 2013. “A unified approach to model elasto-viscoplastic thixotropic yield-stress materials and apparent yield-stress fluids”. *Rheologica Acta*, Vol. 52, No. 7, pp. 673–694.

de Souza Mendes, P.R.S. and Dutra, E.S.S., 2004. “Viscosity Function for Yield-Stress Liquids OVERVIEW OF THE AVAILABLE VISCOSITY”. Vol. 14, No. 6, pp. 296–302.

Fraggedakis, D., Dimakopoulos, Y. and Tsamopoulos, J., 2016. “Yielding the yield stress analysis: A thorough comparison of recently proposed elasto-visco-plastic (EVP) fluid models”. *Journal of Non-Newtonian Fluid Mechanics*, Vol. 236, pp. 104–122.

Franca, L.P. and Frey, S.L., 1992. “Stabilized finite element methods: II. The incompressible Navier-Stokes equations”. *Computer Methods in Applied Mechanics and Engineering*, Vol. 99, No. 2-3, pp. 209–233.

Gueslin, B., Talini, L., Herzhaft, B., Peysson, Y. and Allain, C., 2006. “Flow induced by a sphere settling in an aging yield-stress fluid”. *Physics of Fluids*, Vol. 18, No. 10.

Link, F.B., Frey, S., Thompson, R.L., Naccache, M.F. and de Souza Mendes, P.R., 2015. “Plane flow of thixotropic elasto-viscoplastic materials through a 1:4 sudden expansion”. *Journal of Non-Newtonian Fluid Mechanics*, Vol. 220, pp. 162–174.

López-Aguilar, J.E., Webster, M.F., Tamaddon-Jahromi, H.R. and Manero, O., 2014. “A new constitutive model for worm-like micellar systems - Numerical simulation of confined contraction-expansion flows”. *Journal of Non-Newtonian Fluid Mechanics*, Vol. 204, pp. 7–21.

López-Aguilar, J.E., Webster, M.F., Tamaddon-Jahromi, H.R. and Manero, O., 2016. “A comparative numerical study of time-dependent structured fluids in complex flows”. *Rheologica Acta*, Vol. 55, No. 3, pp. 197–214.

López-Aguilar, J., Webster, M., Tamaddon-Jahromi, H. and Manero, O., 2018. “Predictions for circular contraction-expansion flows with viscoelastoplastic & thixotropic fluids”. *Journal of Non-Newtonian Fluid Mechanics*, Vol. 261, pp. 188–210.

Mahmood, R., Kousar, d.n., Yaqub, M. and Jabeen, K., 2017. “Numerical simulations of the square lid driven cavity flow of bingham fluids using nonconforming finite elements coupled with a direct solver”. *Advances in Mathematical Physics*, Vol. 2017, pp. 1–10.

Nassar, B., de Souza Mendes, P.R. and Naccache, M.F., 2011. “Flow of elasto-viscoplastic liquids through an axisymmetric expansion-contraction”. *Journal of Non-Newtonian Fluid Mechanics*, Vol. 166, No. 7-8, pp. 386–394.

Oishi, C.M., Martins, F.P. and Thompson, R.L., 2017. “The "avalanche effect" of an elasto-viscoplastic thixotropic material on an inclined plane”. *Journal of Non-Newtonian Fluid Mechanics*, Vol. 247, pp. 165–177.

Oishi, C.M., Martins, F.P. and Thompson, R.L., 2020. “Gravitational effects in the collision of elasto-viscoplastic drops on a vertical plane”. *Fluids*, Vol. 5, No. 2, p. 61.

Park, Y.S. and Liu, P.L.F., 2010. “Oscillatory pipe flows of a yield-stress fluid”. *Journal of Fluid Mechanics*, Vol. 658, pp. 211–228.

Putz, A.M., Burghelea, T.I., Frigaard, I.A. and Martinez, D.M., 2008. “Settling of an isolated spherical particle in a yield stress shear thinning fluid”. *Physics of Fluids*, Vol. 20, No. 3, pp. 1–12.

Rajagopalan, D., Armstrong, R.C. and Brown, R.A., 1990. “Finite element methdos for calculation of steady, viscoelastic flow using constitutive equations with a newtonian viscosity”. *Journal of Non-Newtonian Fluid Mechanics*, Vol. 36, pp. 159 – 192.

Santos, D., Frey, S., Naccache, M. and De Souza Mendes, P., 2014. “Flow of elasto-viscoplastic liquids through a planar expansion-contraction”. *Rheologica Acta*, Vol. 53.

Saramito, P., 2007. “A new constitutive equation for elastoviscoplastic fluid flows”. *Journal of Non-Newtonian Fluid Mechanics*, Vol. 145, No. 1, pp. 1–14.

Saramito, P., 2009. “A new elastoviscoplastic model based on the Herschel-Bulkley viscoplastic model”. *Journal of Non-Newtonian Fluid Mechanics*, Vol. 158, No. 1-3, pp. 154–161.

Sikorski, D., Tabuteau, H. and de Bruyn, J.R., 2009. “Motion and shape of bubbles rising through a yield-stress fluid”. *Journal of Non-Newtonian Fluid Mechanics*, Vol. 159, No. 1-3, pp. 10–16.